

Dynamic Modeling of Human Complement System using Reduced Ordered Models

Adithya Sagar, Wei Dai[#], Mason Minot[#], and Jeffrey D. Varner^{*}

School of Chemical and Biomolecular Engineering

Cornell University, Ithaca NY 14853

Running Title: Dynamic Modeling of Human Complement System using Reduced Ordered Models

To be submitted: ???????

[#] Denotes equal contribution

^{*}Corresponding author:

Jeffrey D. Varner,

Professor, School of Chemical and Biomolecular Engineering,

244 Olin Hall, Cornell University, Ithaca NY, 14853

Email: jdv27@cornell.edu

Phone: (607) 255 - 4258

Fax: (607) 255 - 9166

Abstract

Fill me in.

Keywords: Biochemical engineering, systems biology, reduced order models, complement system

1 Introduction

2 Complement is a central part of innate immunity and plays a very significant role in reg-
3 ulating the inflammatory response. Complement was first discovered in the 1890s where
4 it was found to 'complement' the bactericidal activity of natural antibodies. Complement
5 is mediated through a set of approximately 30-35 soluble and cell surface proteases.
6 The central process in complement activation involves the formation of Membrane Attack
7 Complex (MAC) and a protein called C5a. C5a acts as a bridge between innate and adap-
8 tive immunity and plays a very important role in regulating inflammation and coagulation.
9 Complement activation takes places through three different pathways: the alternate, the
10 classical and the lectin. Each of these pathways involves a different initiator signal that
11 leads to the formation of a serine protease called C5 convertase which cleaves an in-
12 active protein called C5 to form C5a and C5b. The classical pathway is triggered when
13 antibodies form complexes with foreign antigens or other pathogens. A multimeric pro-
14 tein complex C1 binds to the antigen-antibody complex and undergoes a conformational
15 change. This activated complex cleaves proteins C4 and C2 to C4a, C4b, C2a and C2b
16 respectively. C4a and C2b combine to form a protease C4bC2a also known as the classi-
17 cal C3 convertase. The lectin pathway is initiated through the binding of L-ficolin or Man-
18 nose Binding Lectin (MBL) to the carbohydrates on the surfaces of bacterial pathogens.
19 This bound complex in turn cleaves C4 and C2 and leads to the production of C4bC2a.
20 The alternate pathway involves a 'tickover' mechanism in which a protein called C3 is hy-
21 drolyzed to form C3b. In presence of foreign pathogens C3b binds to these surfaces and
22 recruits additional factors called factor B and factor D that lead to the formation of alter-
23 nate C3 convertase - C3bBb. The formation of classical and alternate C3 convertases on
24 bacterial surfaces is followed by the formation of proteases called C5 convertases. The
25 classical and alternate C3 convertases recruit C3, Factor B and Factor D to form classical
26 C5 convertase (C4bC2aC3b) and alternate C5 convertase (C3bBbc3B) respectively. The

C5 convertases then cleave C5 to form C5a and C5b respectively. The cleavage of C5 is followed by a series of sequential cleavages of proteins C6, C7, C8 and C9 that combine with C5b to form the MAC complex. The activation of complement and formation of C5a and MAC complex is regulated at different points through a number of plasma and host cell proteins. C4 binding protein (C4BP), — (NEEDS TO BE FILLED)

Given the complexity and importance of complement, developing mathematical models of complement are crucial to understanding its dynamics. Complement models have typically been formulated as linear or non-linear Ordinary Differential Equation (ODE) systems. Hirayama et al. (ref) used a system of linear ODEs to model the classical pathway of complement. Korotaevskiy and co-workers (ref) built a theoretical model of complement using a system of non-linear ODEs that included classical, lectin and alternate pathways. However both these studies involve no validation studies with experimental data. Liu et al used analyzed the formation of classical and lectin C3 convertases and the regulatory role of C4BP using a system of 45 non-linear ODEs with 85 parameters. Recently, Zewde and co-workers built a detailed mechanistic model of alternative complement activation was built using 107 ODEs and 74 kinetic parameters (Ref). This model delineated the response of complement on a host cell and a foreign antigen. However, these previous models were largely based upon mechanistic knowledge. However given the complexity of complement and its interactions with other networks like coagulation, autonomous nervous system, adaptive immunity it is unfeasible and computationally expensive to build such large mechanistic models. In addition is much more difficult to experimentally interrogate the response of various complement proteins under different conditions. This also presents with the problem of estimation of a large number of parameters with little or no experimental data. Thus there exists a need to reduce the mechanistic complexity while capturing dynamics of complement accurately.

In this study, we formulated a hybrid modeling of the human complement system. [FILL

53 ME IN].

Results

Formulation of a reduced order complement model. We developed a reduced order extrinsic human complement network consisting of the most crucial steps of the human complement system (Fig. 1). The core of our model was based upon the experimental measurements of Morad and coworker's earlier work [1], we only consider the activation of complement system through the alternate and the lectin pathways. In doing so we aim to capture a complex biological phenomenon using a few simple ordinary differential equations. A trigger event initiates the lectin pathway in the presence of zymosan, which activates the cleavage of $C2$ and $C4$ into $C2a$ and $C2b$, and $C4a$ and $C4b$ respectively. Classical Pathway (CP) $C3convertase$ ($C4aC2b$) is by the combination of $C4a$ and $C2b$, which catalyzes the cleavage of $C3$ into $C3a$ and $C3b$. Similarly, the activation of the alternative pathways happens through the spontaneous hydrolysis of $C3$ which facilitates the cleavage of $C3$. $C3b$ then could combine with with $C3$ to form alternate pathway (AP) $C3convertase$. The both versions of the $C3convertase$ catalyzes the cleavage of $C3$ into $C3a$ and $C3b$, and $C3b$ can then combine with either CP or APC3convertase to form $C5convertase$, CP or AP respectively that is responsible for the cleavage of $C5$ to $C5a$ and $C5b$. Lectin pathway activation was approximated using a combination of saturation kinetics and Hill-like function control functions. These control coefficients then modified the rates of model processes at each time step. Hill-like transfer functions $0 \leq f(\mathbf{Z}) \leq 1$ quantified the contribution of components upon a target process, in this study, \mathbf{Z} represents the abundance of the initiator. Taken together, while the reduced order human complement model encodes significant biological complexity, it is highly compact (consisting of only 18 differential equations). Thus, it will serve as an excellent proof of principle example to study the reduction of a highly complex human subsystem.

Model were estimated using dynamically dimensioned search. A critical challenge for any dynamic model is the estimation of kinetic parameters. We estimated kinetic and

control parameters in a hierarchical fashion using two *in vitro* time-series human complement data sets with and without zymosan present. The residual between simulation and experimental measurements were minimized using dynamically dimensioned search (DDS). An initial parameter set was initialized with randomized kinetic and control parameters and allowed to search for parameter vectors that minimized the residual. Knowing that the kinetic and control parameters of the lectin pathway does not affect the dynamics of the alternate pathway, we used a hierarchal approach that estimated the parameters for the alternative pathway and lectin pathway separately. For the alternative pathway, we utilized the time-course experimental measurements of Morad and coworkers [1] of *C3a* and *C5a* in the absence of zymosan and only allowed the alternative parameters to vary (Fig. 2 A and B). The estimated alternate parameters was then fixed for the determination of lectin pathway parameters. The training for the lectin parameters, we used the experimental measurements of *C3a* and *C5a* in the presence of 1 g of zymosan published by Morad et al [1] (Fig. 2 C and D).

The reduced human complement model captured the behavior of the alternative and lectin pathways through the time-course abundance of *C3a* and *C5a* (Fig. 2). However we were not able to capture the curvature of the *C5a* alternate (Fig. 2), the decreasing slope of the experimental measurements may be an indication of the decreasing cofactors that are required for the spontaneous hydrolysis in the alternative pathway, which we neglected. Taken together, the model identification results suggested that our reduced order approach could reproduce a panel of lectin pathway initiation data sets in the neighborhood of physiological factor and inhibitor concentrations. However, it was unclear whether the reduced order model could predict new data, without updating the model parameters.

Validation of the reduced order human complement model. We tested the predictive power of the reduced order human complement model with validation data sets not used during model training. Six validation data sets were used, three for *C3a* and *C5a*

respectively at different zymosan concentrations. All kinetic and control parameters were fixed for the validation simulations. The reduced order model predicted the $C3a$ and $C5a$ time-course profiles at a qualitative level (Fig. 3).

Global Sensitivity analysis of the reduced order complement model We conducted a Sobol's sensitivity analysis to estimate which parameters controlled the performance of the reduced order model. We calculated the sensitivity of the change in $C3a$ and $C5a$ profiles using the residuals between simulation and experimentally measured data for the cases of 0 and 1g zymosan (Fig. 4). For the cases in absence of zymosan where only the alternative pathway is active, we observed that only a few variables are responsible for the system response. For $C3a$ alternate, the sensitivity analysis found that $k_{c3b\text{ basal}}$ and $k_{degradationC3a}$ are the only sensitive parameters. This gives us new insight in which of the parameters play a role in complement activation. Even though $AP\ C3\ Convertase$ is also responsible in the conversion of $C3$ and the production of $C3a$, the kinetic parameters that govern the equation was not sensitive at all. This elucidated that the activation of alternative pathway is more heavily governed by the spontaneous hydrolysis of $C3$ rather than the activity of $AP\ C3\ Convertase$. Surprisingly, closely examining the sensitive parameters that control $C5a$, in addition to the expected kinetic and control parameters related to the formation of $AP\ C5\ Convertase$, we observed that $k_{C3\ Convertase2}$, the was previously not sensitive to $C3a$, to be sensitive in the formation of $C5a$. The $AP\ C3\ Convertase$ is a substrate required for the formation of $AP\ C5\ Convertase$ and the formation of $C3b$. The change in activity of $APC3Convertase$ will not drastically change the $C3a$ dynamics, but will effect $AP\ C5a\ Convertase$ formation and $C5a$ formation. The our reduced order human complement model in combination with Sobol's sensitivity analysis was able to unravel important indirect parameter interaction.

Our sensitivity analysis yielded expected results for the lectin pathway analyzes (Fig. 4 (C and D)). One key difference that was observed between the sensitivity of the pa-

rameters between $C3a$ and $C5a$ was their respective degradation terms. The degradation constant of $C3a$ was sensitive between the two different cases of zymosan that was tested while the degradation constant of the $C5a$ was not sensitive. We believe this difference is attributed to the magnitude of the parameters and their respective concentrations.

Discussion

The discussion has three (sometimes four) paragraphs:

1. **First paragraph:** Present a modified version of the last paragraph of the introduction. In this study, [...]. Taken together, [killer statement]
2. **Second paragraph:** Contrast the key findings of the study with other computational/experimental studies
3. **Third paragraph:** Present future directions. If you had more time, what would like to do? Highlight the key shortcomings of the approach and how will we address them in the future. In this case, we will have a scaling issue if we extend to genome scale. We should extend to dynamic cases, and we need to experimentally validate the findings.

Materials and Methods

We used ordinary differential equations (ODEs) to model the time evolution of proteins (x_i) in our reduced order complement model:

$$\frac{dx_i}{dt} = \sum_{j=1}^{\mathcal{R}} \sigma_{ij} r_j(\mathbf{x}, \epsilon, \mathbf{k}) \quad i = 1, 2, \dots, \mathcal{M} \quad (1)$$

where \mathcal{R} denotes the number of reactions, \mathcal{M} denotes the number of protein species in the model. The quantity $r_j(\mathbf{x}, \epsilon, \mathbf{k})$ denotes the rate of reaction j . Typically, reaction j is a non-linear function of biochemical species abundance, as well as unknown kinetic parameters \mathbf{k} ($\mathcal{K} \times 1$). The quantity σ_{ij} denotes the stoichiometric coefficient for species i in reaction j . If $\sigma_{ij} > 0$, species i is produced by reaction j . Conversely, if $\sigma_{ij} < 0$, species i is consumed by reaction j , while $\sigma_{ij} = 0$ indicates species i is not connected with reaction j . The system material balances were subject to the initial conditions $\mathbf{x}(t_o) = \mathbf{x}_o$, which were specified by the experimental setup and human serum complement protein levels.

Each reaction rate was written as either the product of two terms, a kinetic term (\bar{r}_j) and a control term (f_j), or \bar{r}_j for the case $f_j = 1$:

$$r_j(\mathbf{x}, \epsilon, \mathbf{k}) = \bar{r}_j f_j \quad (2)$$

Each control term, $f_j(\mathcal{Z})$ took the form:

$$f_j(\mathcal{Z}_j, \alpha_j) = \frac{\mathcal{Z}_j^\eta}{\mathcal{Z}_j^\eta + \alpha_j^\eta} \quad (3)$$

where \mathcal{Z}_j denotes the abundance of the j factor (e.g., initiator abundance), α_j denotes the species gain parameter, and η a cooperativity parameter (similar to a Hill coefficient).

We used saturation kinetics to model the lectin pathway activation and C3 and C5

164 convertase activity reaction terms \bar{r}_j :

$$\bar{r}_j = k_j^{max} \epsilon_i \left(\frac{x_s^\eta}{K_{js}^\eta + x_s^\eta} \right) \quad (4)$$

165 where k_j^{max} denotes the maximum rate for reaction j , ϵ_i denotes the enzyme abundance
 166 which catalyzes reaction j , η denotes a cooperativity parameter (similar to a Hill coeffi-
 167 cient), and K_{js} denotes the saturation constant for species s in reaction j .

168 We used mass action kinetics to model the protein conversion reactions within the
 169 network \bar{r}_j :

$$\bar{r}_j = k_j^{max} \epsilon_i \prod_{s \in m_j^-} x_s \quad (5)$$

170 where k_j^{max} denotes the maximum rate for reaction j , ϵ_i denotes the enzyme abundance
 171 which catalyzes reaction j . The product in
 172 Equation (5) was carried out over the set of *reactants* for reaction j (denoted as m_j^-).

173 Applying the general framework to the reduced coagulation network resulted in 18

174 ordinary differential equations, 12 rate equations, and two control equations:

$$\frac{dx_1}{dt} = -r_{init,c4}f_{init,c4} \quad (6)$$

$$\frac{dx_2}{dt} = -r_{init,c2}f_{init,c2} \quad (7)$$

$$\frac{dx_3}{dt} = r_{init,c4}f_{init,c4} \quad (8)$$

$$\frac{dx_4}{dt} = r_{init,c4}f_{init,c4} - r_{cp,c3c,form} \quad (9)$$

$$\frac{dx_5}{dt} = r_{init,c2}f_{init,c2} - r_{cp,c3c,form} \quad (10)$$

$$\frac{dx_6}{dt} = r_{init,c2}f_{init,c2} \quad (11)$$

$$\frac{dx_7}{dt} = r_{c3,basal} - r_{cp,c3c,c3b} - r_{ap,c3c,c3b} \quad (12)$$

$$\frac{dx_8}{dt} = r_{c3,basal} + r_{cp,c3c,c3b} + r_{ap,c3c,c3b} - k_{deg,c3a} * C3a \quad (13)$$

$$\frac{dx_9}{dt} = r_{c3,basal} + r_{cp,c3c,c3b} + r_{ap,c3c,c3b} - r_{ap,c3c,form} \quad (14)$$

$$\frac{dx_{10}}{dt} = r_{cp,c3c,form} - r_{cp,c5c,form} - r_{cp,c3c,c4bp,inhib} \quad (15)$$

$$\frac{dx_{11}}{dt} = r_{ap,c3c,form} - r_{ap,c5c,form} - r_{ap,c3c,factorH,inhib} \quad (16)$$

$$\frac{dx_{12}}{dt} = r_{cp,c5c,form} - r_{cp,c5c,c4bp,inhib} \quad (17)$$

$$\frac{dx_{13}}{dt} = r_{cp,c5c,form} \quad (18)$$

$$\frac{dx_{14}}{dt} = -r_{cp,c5c,c5b} - r_{ap,c5c,c5b} \quad (19)$$

$$\frac{dx_{15}}{dt} = r_{cp,c5c,c5b} + r_{ap,c5c,c5b} - k_{deg,c5a} \quad (20)$$

$$\frac{dx_{16}}{dt} = r_{cp,c5c,c5b} + r_{ap,c5c,c5b} \quad (21)$$

$$\frac{dx_{17}}{dt} = -r_{cp,c3c,c4bp,inhib} - r_{cp,c5c,c4bp,inhib} \quad (22)$$

$$\frac{dx_{18}}{dt} = -r_{ap,c3c,factorH,inhib} \quad (23)$$

$$(24)$$

where

$$\begin{aligned}
 fx = f(&Zymosan, C2, C2a, C2b, C4, C4a, C4b, C3, C3a, C3b, CPC3CConvertase, \dots \\
 &APC3Convertase, CPC5Convertase, APC5Convertase, C5, C5a, \dots \\
 &\dots C5b, C4BP, FactorH)^T \quad (25)
 \end{aligned}$$

The various rate and control equations are given by:

$$r_{init,c4} = \frac{k_{init,c4} * C4}{K_{init,c4,s} + C4} \quad (26)$$

$$r_{init,c2} = \frac{k_{init,c2} * C2}{K_{init,c2,s} + C2} \quad (27)$$

$$f_{init,c4} = \frac{Zymo^{\eta_{zymo,c4}}}{Zymo^{\eta_{zymo,c4}} + \alpha_{c2}^{\eta_{zymo,c4}}} \quad (28)$$

$$f_{init,c2} = \frac{Zymo^{\eta_{zymo,c2}}}{Zymo^{\eta_{zymo,c2}} + \alpha_{c4}^{\eta_{zymo,c2}}} \quad (29)$$

$$r_{c3,basal} = k_{c3b,basal} * C3 \quad (30)$$

$$r_{cp,c3c,c3b} = \frac{k_{cp,c3c} * CP, C3C * C3^{\eta_{cp,c3c}}}{K_{cp,c3c,s}^{\eta_{cp,c3c}} + C3^{\eta_{cp,c3c}}} \quad (31)$$

$$r_{ap,c3c,c3b} = \frac{k_{ap,c3c} * AP, C3C * C3}{K_{ap,c3c,s} + C3} \quad (32)$$

$$r_{cp,c3c,form} = k_{cp,c3c,form} * C4b * C2a \quad (33)$$

$$r_{ap,c3c,form} = k_{ap,c3c,form} * C4b * C2a \quad (34)$$

$$r_{cp,c3c,c4bp,inhib} = k_{cp,c3c,inhib} * CP, C3C * C4b * C4BP \quad (35)$$

$$r_{ap,c3c,factorH,inhib} = k_{ap,c3c,inhib} * AP, C3C * FactorH \quad (36)$$

$$r_{cp,c5c,form} = k_{cp,c5c,form} * CP, C3C * C3b \quad (37)$$

$$r_{ap,c5c,form} = k_{ap,c5c,form} * AP, C3C * C3b \quad (38)$$

$$r_{cp,c5c,c5b} = \frac{k_{cp,c5c} * CP, C5C * C5^{\eta_{cp,c5c}}}{K_{cp,c5c,s}^{\eta_{cp,c5c}} + C5^{\eta_{cp,c5c}}} \quad (39)$$

$$r_{ap,c5c,c5b} = \frac{k_{ap,c5c} * AP, C5C * C5}{K_{ap,c5c,s} + C5} \quad (40)$$

$$r_{cp,c5c,c4bp,inhib} = k_{cp,c5c,inhib} * CP, C5C * C4BP \quad (41)$$

0.1 Estimation of Model Parameters From Experimental Data - Needs to be completed Model parameters were estimated by minimizing the difference between simula-

178 tions and experimental C3a and C5a measurements (squared residual):

$$\min_{\mathbf{k}} \sum_{\tau=1}^{\mathcal{T}} \sum_{j=1}^{\mathcal{S}} \left(\frac{\hat{x}_j(\tau) - x_j(\tau, \mathbf{k})}{\omega_j(\tau)} \right)^2 \quad (42)$$

179 where $\hat{x}_j(\tau)$ denotes the measured value of species j at time τ , $x_j(\tau, \mathbf{k})$ denotes the
 180 simulated value for species j at time τ , and $\omega_j(\tau)$ denotes the experimental measurement
 181 variance for species j at time τ . The outer summation is with respect to time, while the
 182 inner summation is with respect to state. We minimized the model residual using Particle
 183 swarm optimization (PSO) [?]. PSO uses a *swarming* metaheuristic to explore parameter
 184 spaces. A strength of PSO is its ability to find the global minimum, even in the presence of
 185 potentially many local minima, by communicating the local error landscape experienced
 186 by each particle collectively to the swarm. Thus, PSO acts both as a local and a global
 187 search algorithm. For each iteration, particles in the swarm compute their local error by
 188 evaluating the model equations using their specific parameter vector realization. From
 189 each of these local points, a globally best error is identified. Both the local and global
 190 error are then used to update the parameter estimates of each particle using the rules:

$$\Delta_i = \theta_1 \Delta_i + \theta_2 \mathbf{r}_1 (\mathcal{L}_i - \mathbf{k}_i) + \theta_3 \mathbf{r}_2 (\mathcal{G} - \mathbf{k}_i) \quad (43)$$

$$\mathbf{k}_i = \mathbf{k}_i + \Delta_i \quad (44)$$

191 where $(\theta_1, \theta_2, \theta_3)$ are adjustable parameters, \mathcal{L}_i denotes the local best solution found by
 192 particle i , and \mathcal{G} denotes the best solution found over the entire population of particles.
 193 The quantities r_1 and r_2 denote uniform random vectors with the same dimension as the
 194 number of unknown model parameters
 195 ($\mathcal{K} \times 1$). In this study, we used $(\theta_1, \theta_2, \theta_3) = (1.0, 0.05564, 0.02886)$. The quality of pa-
 196 rameter estimates was measured using goodness of fit (model residual). The particle

swarm optimization routine was implemented in the Python programming language. All plots were made using the Matplotlib module of Python [?].

0.2 Global Sensitivity Analysis of Model Performance

We conducted a global sensitivity analysis, using the variance-based method of Sobol, to estimate which parameters controlled the performance of the reduced order model [?]. We computed the total sensitivity index of each parameter relative to four performance objectives, each objective was based on the sum of squared errors between model and experimental data for C3a alternate, C5a alternate, C3a lectin, and C5a lectin simulations. We established the sampling bounds for each parameter from the minimum and maximum value of that parameter in the parameter set ensemble. We used the sampling method of Saltelli *et al.* [?] to compute a family of $N(2d + 2)$ parameter sets which obeyed our parameter ranges, where N was the number of trials, and d was the number of parameters in the model. In our case, $N = 200$ and $d = 42$, so the total sensitivity indices were computed from 11,600 model evaluations. The variance-based sensitivity analysis was conducted using the SALib module encoded in the Python programming language [2].

²¹² **Acknowledgements**

²¹³ This study was supported by an award from [FILL ME IN].

References

1. Morad HO, Belete SC, Read T, Shaw AM (2015) Time-course analysis of c3a and c5a quantifies the coupling between the upper and terminal complement pathways in vitro. Journal of immunological methods 427: 13–18.
2. Herman J. Salib: Sensitivity analysis library in python (numpy). contains sobol, morris, fractional factorial and fast methods. available online: <https://github.com/jdherman/salib>.

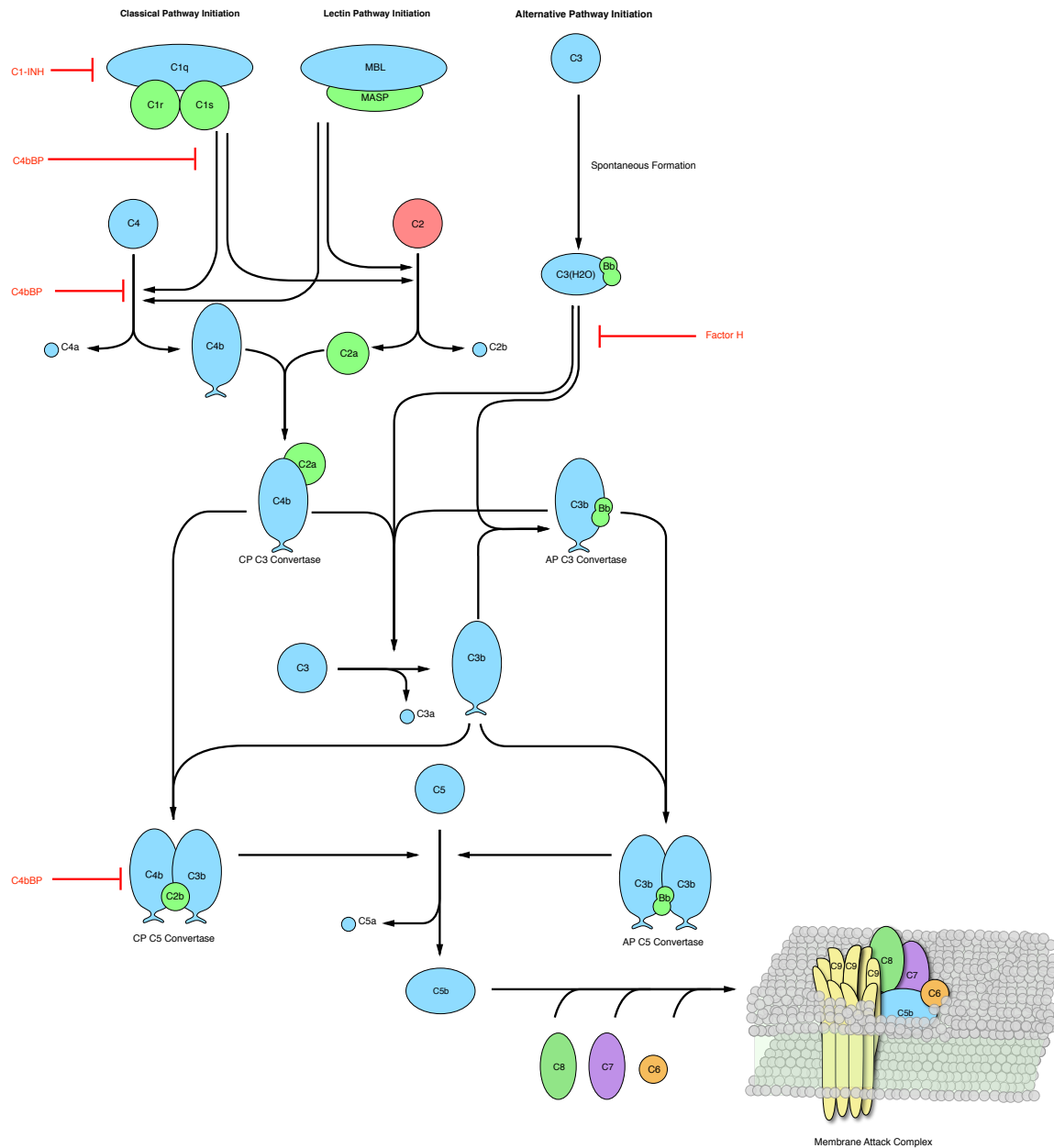


Fig. 1: Simplified schematic representation of the human complement system. The complement cascade is activated through any one, or more, of the three pathways: classical, lectin, and alternate pathway. The classical pathway is activated by the complex formation of *C1q*, *C1r*, and *C1s* by the recognition of antibody:antigen complexes. Similarly, the lectin pathway is initiated by binding mannan-binding lectin to mannose on pathogen surfaces. Lastly, the alternative pathway is activated when a complement component is spontaneously bound to the surface of the pathogen or virus. The activation from the three pathways creates a cascade of reactions that forms the proteases, *C3* Convertase that cleaves *C3* into *C3a*, and *C3b*, the main effector molecule of the complement system. *C3b* can find to a *C3* convertase and form a *C5* convertase that cleaves *C5* into *C5a*, and *C5b* that undergoes a series of reactions to form the membrane attack complex (*MAC*).

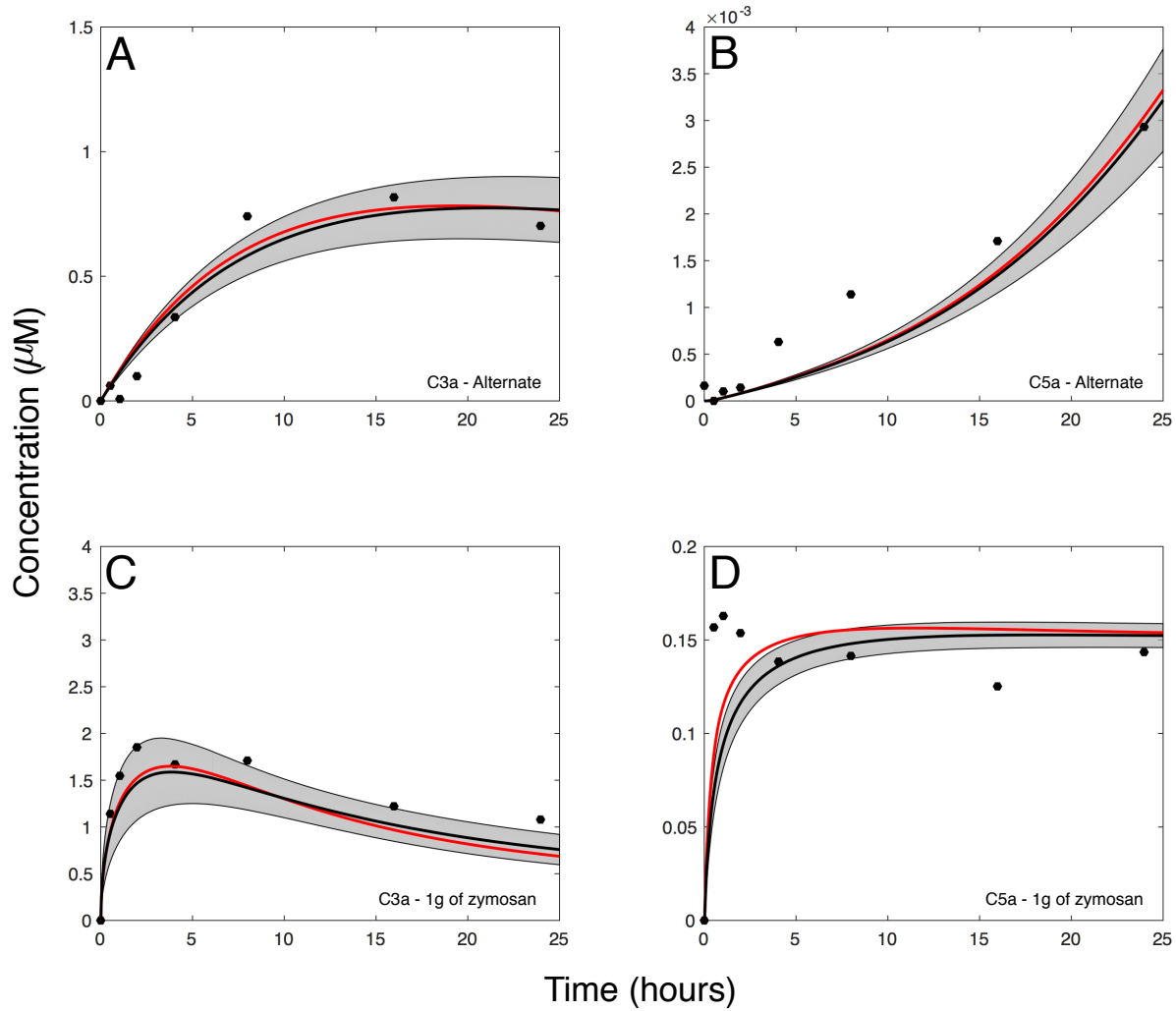


Fig. 2: Reduced order complement model training simulation for lectin and alternative pathway in presence of zymosan. Reduced order complement model parameters were estimated using dynamically dimensioned search (DDS) [Tolson and Shoemaker,2007,WRR] using the availability of zymosan as a function of lectin pathway initiation. Only parameters that govern the behavior of alternative pathway were allowed to vary when zymosan was not present. Our model training was conducted in a hierarchal fashion where the alternate parameters were trained and then used and fixed in estimating the lectin parameters. The red line shows the best-fit parameter, the black lines denotes the simulated mean value of $C3a$ or $C5a$ for a 50 parameter set ensemble. The shaded region denotes the distribution of $C3a$ and $C5a$ of the ensemble.

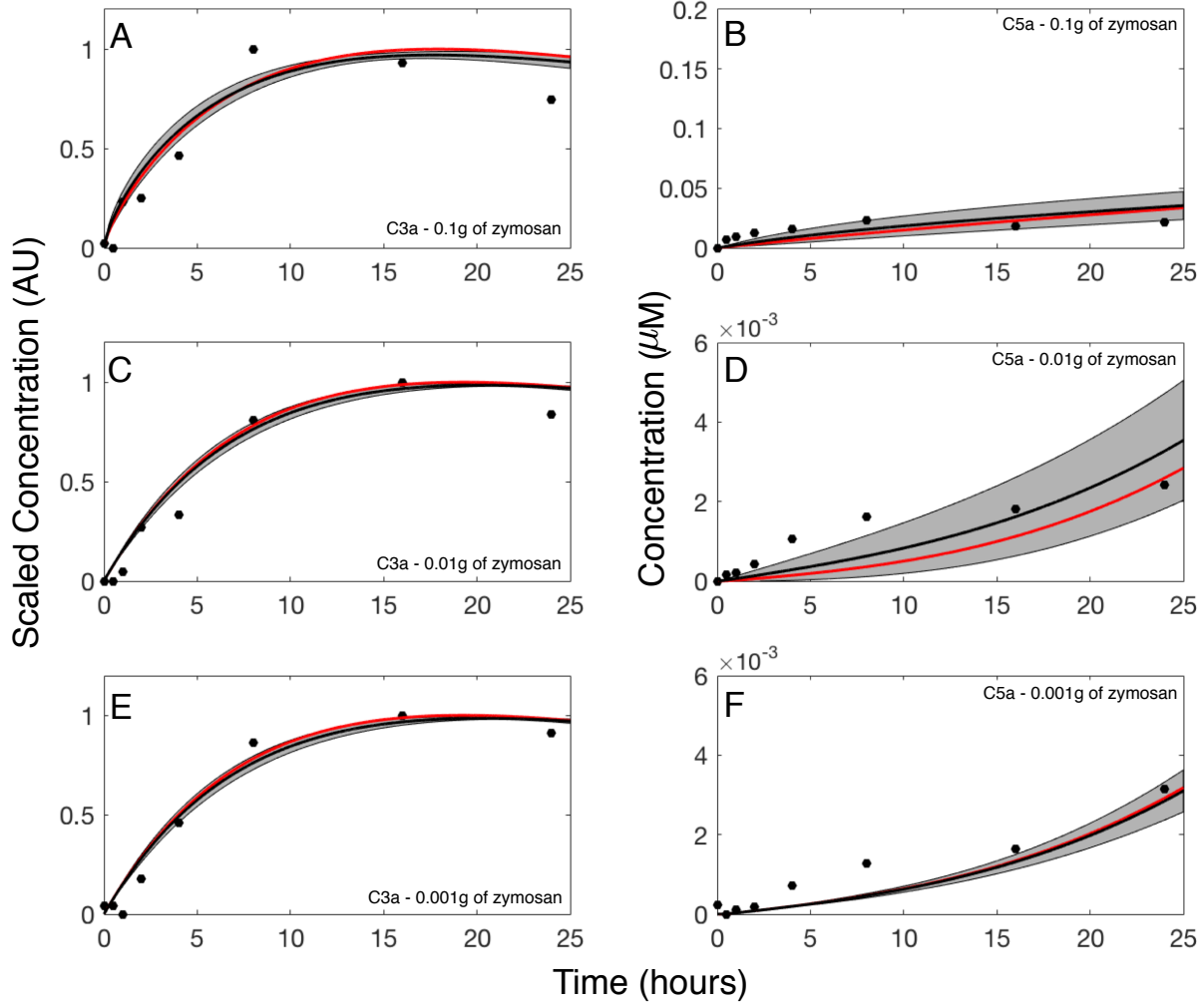


Fig. 3: Reduced order complement model predictions of lectin and alternative pathway in presence of zymosan. (A-F) Simulation of complement dynamics in the presence of zymosan were conducted for a range of trigger values (0.1, 0.01, and 0.001 grams of zymosan). The time-course profiles of *C3a* and *C5a* under three different zymosan concentrations were simulated using 50 ensembles of trained parameter sets against experimental data of Shaw et al [REF]. The red curve represents the best fit parameter, grey shaded region denotes the prediction results from 50 ensembles of parameter sets, and the black curve is the mean of the ensemble. All complement protein and factor initial concentrations coincided with human serum levels unless otherwise noted.

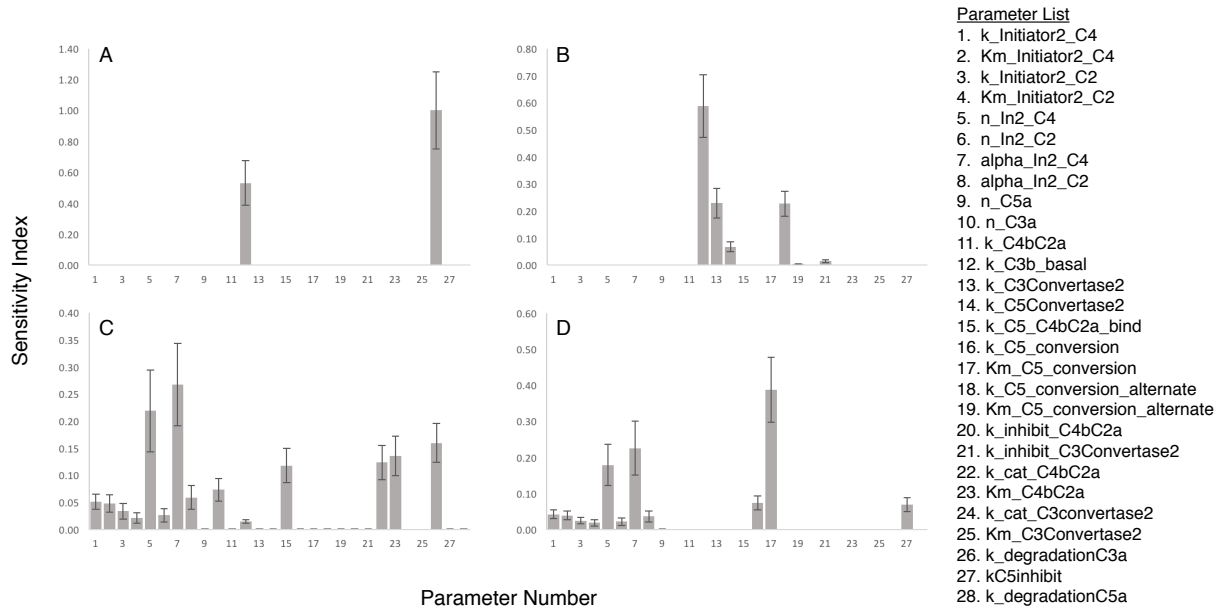


Fig. 4: Sobol's sensitivity analysis of the reduced order complement model with respect to the modeling parameters. Sensitivity analysis was conducted on the four cases we used to train our model: (A) C3a at 0 zymosan, (B) C5a 0 zymosan, (C) C3a 1 g zymosan, and (D) C5a 1 g zymosan. The bars denote total sensitivity index which includes local contribution of each parameter and global sensitivity of significant pairwise interactions. The error bars are the 95 percent confidence interval. k represents association rate, km denote Michaelis-Menten saturation constants, and α and n refers to the exponentials of the control functions.

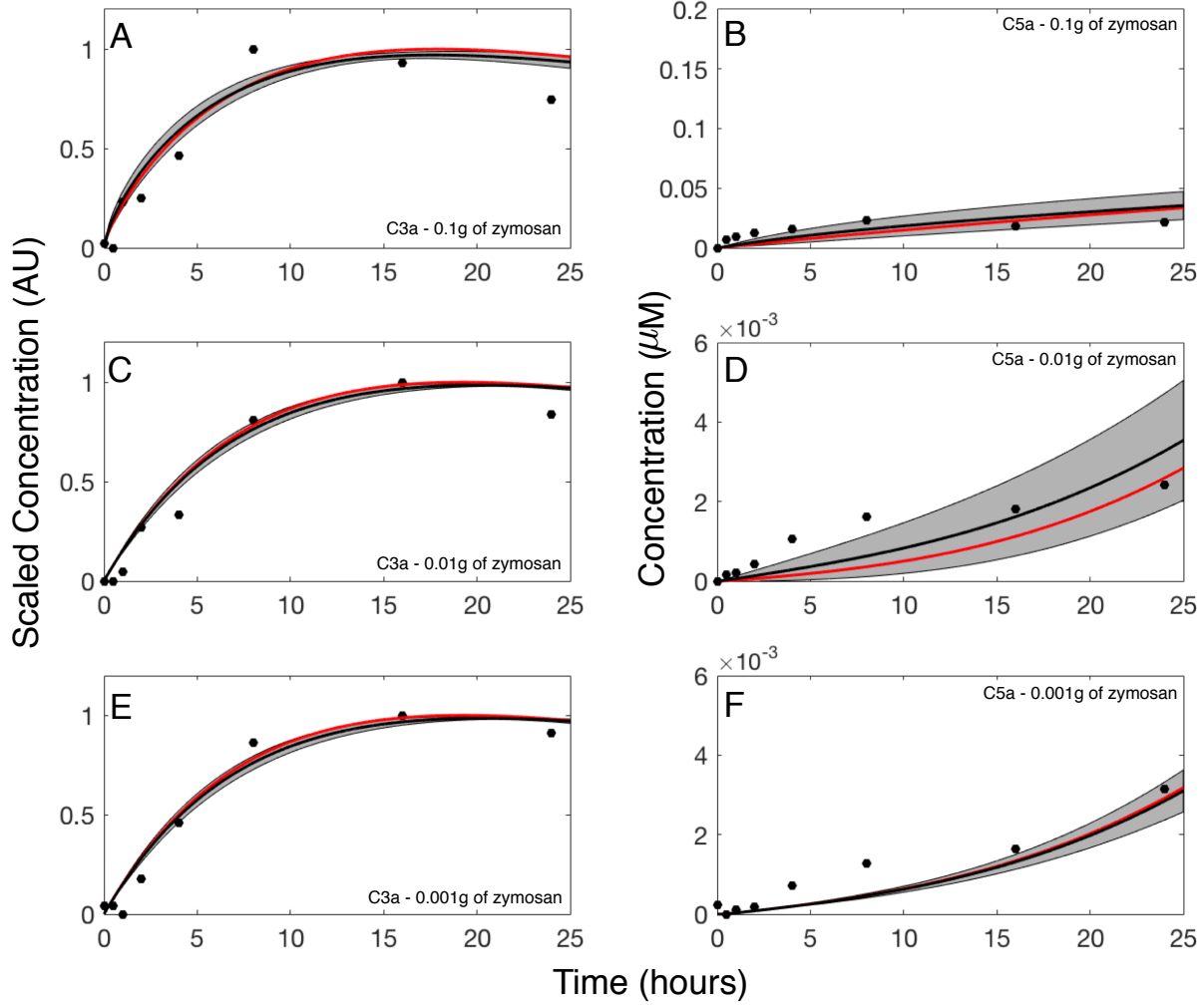


Fig. 5: Reduced order complement model predictions of lectin and alternative pathway in presence of zymosan. (A-F) Simulation of complement dynamics in the presence of zymosan were conducted for a range of trigger values (0.1, 0.01, and 0.001 g zymosan). The time-course profiles of *C3a* and *C5a* under three different zymosan concentrations were simulated using 50 ensembles of trained parameter sets against experimental data of Shaw et al [REF]. The red curve represents the best fit parameter, grey shaded region denotes the prediction results from 50 ensembles of parameter sets, and the black curve is the mean of the ensemble. All complement protein and factor initial concentrations coincided with human serum levels unless otherwise noted.

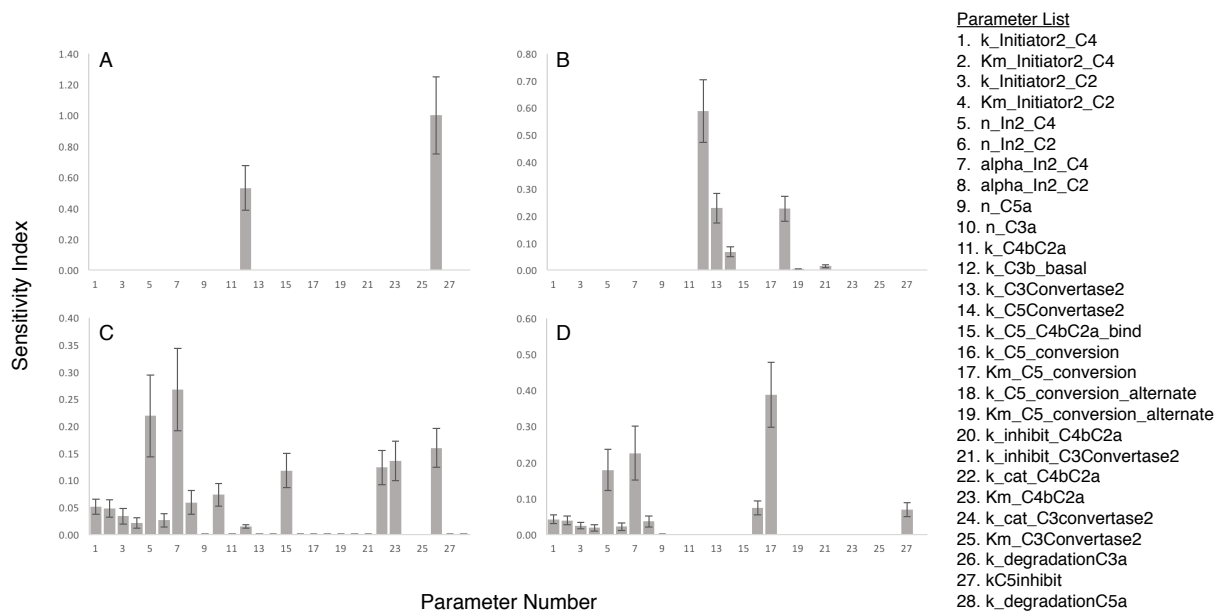


Fig. 6: Sensitivity Analysis